small
NANO MICRO
www.small-journal.com

Aminolated and Thiolated PEG-Covered Gold Nanoparticles with High Stability and Antiaggregation for Lateral Flow Detection of Bisphenol A

Li-Kai Lin, Aytekin Uzunoglu,* and Lia A. Stanciu**

The few lateral flow assays (LFAs) established for detecting the endocrine disrupting chemical bisphenol A (BPA) have employed citrate-stabilized gold nanoparticles (GNPs), which have inevitable limitations and instability issues. To address these limitations, a more stable and more sensitive biosensor is developed by designing strategies for modifying the surfaces of GNPs with polyethylene glycol and then testing their effectiveness and sensitivity toward BPA in an LFA. Without the application of any enhancement strategy, this modified BPA LFA can achieve a naked-eye limit of detection (LOD) of 0.8 ng mL^{-1}, which is 12.5 times better than the LOD of regular BPA LFAs, and a quantitative LOD of 0.472 ng mL^{-1}. This modified LFA has the potential to be applied to the detection of various antigens.

1. Introduction

Bisphenol A (BPA) is an important chemical component of organic materials used in the chemical engineering industry. Over the past several decades, the applications of BPA have been expanding rapidly to include the food industry, the medical field, toy manufacturing, and the consumer products industry. To date, BPA has been primarily applied for fabricating polycarbonate and epoxy resin products.[1–3] The increase in the use of this synthetic chemical has made lives considerably more convenient. However, despite these benefits, challenges have arisen because BPA is also an endocrine disrupting chemical (EDC) and is suspected of being a carcinogen. Low-dose exposure to BPA has adverse health effects on humans.[4–8] Because of its extensive applications, BPA is prevalent in the environment, and human exposure to it is common. Thus, issues related to the food safety of BPA have come into focus. There many potential risks of BPA and its impact are wide ranging because of the ubiquity of products containing BPA. For example, BPA is used to make food and beverage containers and to line metal food cans to prevent corrosion. Numerous studies have reported that BPA can leach out of containers and contaminate the water and food they contain; additionally, it is used in dental fillings and in medical instruments. Moreover, BPA has been discovered in massive quantities on the surface of receipt paper.[9,10] Because of the ubiquity of BPA products and the serious pollution situation in our environment, developing a rapid, economical, highly sensitive, and extremely selective method for detecting BPA is of critical importance.

Current methods for detecting BPA are primarily based on the use of electronic devices, such as high-performance liquid chromatography (HPLC), gas chromatography–mass spectrometry, and Raman spectroscopy.[11–15] These device-based methods are highly sensitive and selective for BPA detection. However, these devices are expensive and require special training to operate, and the tests are time consuming. These disadvantages have prevented them from becoming widespread, making the capacity for on-site detection rare. To facilitate the on-site detection of BPA, aptamer-based methods and enzyme-linked immunosorbent assays (ELISAs) have been broadly investigated and developed.[16–18] The use of aptamers and ELISA has allowed researchers to avoid the expense of purchasing high-cost devices, making tremendous progress on the path toward on-site detection. However, these colorimetric detection methods still involve procedures such as separation and washing steps that must be conducted in specialized laboratories by trained professionals.

To make on-site BPA detection feasible, lateral flow immunoassays (LFIAs), or lateral flow assays (LFAs), are used to eliminate the requirement of in-lab detection. LFAs, an immunochromatographic method, have three operation modes, i.e., competitive, sandwich, and multiplex formats, and combine several concepts into one tiny, convenient device. LFAs have successfully overcome the shortcomings of traditional identification methods, which rely on experiments conducted in labs by trained personnel. LFIAs offer a rapid and inexpensive one-step sample treatment with few interfaces that is portable, highly sensitive, highly selective, and effective in detecting pathogens. In addition to other advantages, the most notable benefit is that LFAs can be performed by untrained operators.[19,20]

L.-K. Lin, Dr. A. Uzunoglu, Prof. L. A. Stanciu
School of Materials Engineering
Neil Armstrong Hall of Engineering
Purdue University
701 West Stadium Avenue, West Lafayette, IN 47907-2045, USA
E-mail: lin688@purdue.edu; aytekingyte@gmail.com; lstanciu@purdue.edu
The ORCID identification number(s) for the author(s) of this article can be found under https://doi.org/10.1002/smll.201702828.

DOI: 10.1002/smll.201702828

Lateral flow (LF) biosensors have been applied to detect a great variety of species, including biomolecules, pathogens, contaminants, and allergens.[20,21] Examples include detecting *Escherichia coli*,[22] progesterone in milk,[23] and the allergen parvalbumin using magnetic nanoparticles.[24] In addition, researchers continue to improve LFAs by augmenting their detection capabilities, developing methods such as enzyme-amplified LFAs for *E. coli* detection[25] and LFAs improved by isotachophoresis.[26]

One of the most important applications of LFAs is the detection of BPA because of the importance of BPA in manufacturing plastics used in food and beverage packaging. People unknowingly encounter BPA every day and are harmed by it. Currently, many instrument-based methods are available for detecting BPA. However, there is a lack of on-site BPA detection methods, and a few studies have focused on detecting BPA using LFAs. The first BPA LFA was developed in 2013.[16] In the same year, an amplified LFA for BPA detection was developed by the same author using two sizes of gold nanoparticles (GNPs) and an extra conjugate pad.[27] In 2014, Maiolini et al. used a similar LFA to detect BPA in water stored in baby bottles.[28]

All of the above studies performed labeling using naked GNPs, which have intrinsic limitations. The main problem with LF detection arises from the aggregation of electrostatically stabilized GNPs.[29] For most LFAs, their fabrication and experimental procedures are conducted in various buffers that require preadjustment to the proper pH value in order to maintain the normal functions of biomolecules. Buffers commonly contain components such as NaCl and KCl that drastically increase the ion concentration in solution and shrink the electrostatic double layers on the GNPs; these layers are used to stabilize GNPs and prevent them from aggregating. In addition, the binding between biorecognition molecules and bare GNPs relies on weaker secondary bonds, such as electrostatic force, hydrophobic forces, and dative bonds.[30] To prevent those molecules from detaching from the surface and disrupting the electrostatic double layers on the GNPs, the pH value, amount, and concentration of the biorecognition probes must be adjusted. Experiments and manufacturing also suffer from repeated washing steps, leading to unsuccessful binding. Furthermore, because the surface of normal GNPs is unprotected and is stabilized by only ions, which are easily replaced and neutralized by foreign molecules, extra blocking sequences and strip pretreatments are also necessary to decrease the possibility of nonselective adsorption. Finally, because BPA is a relatively simple and small chemical with a molecular weight of only 228 Da, it cannot bind to two biorecognition molecules simultaneously; thus, the competitive format has been adopted as the standard assay for BPA LF detection.[16,28] In a competitive assay, reducing the concentration of bioprobes (e.g., antibodies (Abs)) on the labels (e.g., GNPs) is necessary to decrease the limit of detection (LOD) to a lower concentration. This allows antigen molecules (BPA) at lower concentrations in the samples to compete with the antigens (4,4-bis(4-hydroxyphenyl) valeric acid–bovine serum albumin, BHPVA–BSA) on the test line for binding to GNP–Abs in the testing area on the LF strips. However, decreasing the concentration of probes on the labels reduces the color intensity in the testing region. In this case, the deficiencies mentioned above for naked GNPs negatively affect the label and make its signal unclear and unstable, thus complicating the quantification of the antigen. Even when various complicated blocking treatments are applied to the label surface and strips to stabilize the fluctuating signals from the testing area, detecting antigens with low concentrations near the LOD is challenging because for regular GNPs instability and nonselective adsorption are inevitable, leading to unexpected false positives or false negatives.

Stabilizing nanoscale gold is one of the primary problems encountered in most applications of LFAs. There are several prerequisites to maintain their size and shape. When the surrounding environment changes, the stability of GNPs decreases, which significantly affects BPA detection when the competitive format is applied. In previous research on the use of naked GNPs, multiple blocking agents, such as Abs, proteins (e.g., bovine serum albumin), and polymers (e.g., poly(ethylene glycol), PEG), were applied to induce steric hindrance on the GNP surfaces after the bioprobes and GNP conjugates have been assembled, providing extra stability and alleviating the aforementioned challenges with detection.[27,31] However, posttreatment methods still depend on relatively unreliable secondary bonds. The intrinsic problems arise because the use of regular GNPs considerably decreases the accuracy of BPA LFAs, increases the possibility of experimental failure, and raises the potential costs due to the application of expensive biomaterials. Hence, appropriate modification of GNP surfaces involving primary bonds is highly desirable in order to apply GNPs to LFAs. To address the abovementioned concerns, structurally modified derivatives of the versatile polymer PEG should be considered. Because of its amphiphilic nature, PEG is compatible with most samples. The molecular structure of PEG is simple, making the polymer stable and inert.[32] In this study, compared to previous BPA LFAs using regular GNPs, a novel LFA with considerably increased stability and sensitivity for detecting BPA was established using a customized surface-modified antiaggregation GNP as a label. These GNPs comprise a gold core, a thiolated PEG protective cover, and an outmost layer decorated with amine groups. A comparison of the customized GNPs with regular GNPs is shown in **Figure 1**. Coating the surface of naked GNPs with modified PEG through S—Au bonds can impart higher stability and decreased nonselective adsorption to the nanoparticles. In addition, almost completely eliminating label background signals and making the signal in the testing area clearer and more intense clearly increased the sensitivity of the modified BPA LFA. Compared to regular BPA LFAs, the qualification and quantification of BPA with the modified BPA LFA was much more accurate and easier to perform. Notably, because the composition of the modified GNPs successfully prevented them from aggregating in various buffers during the strip fabrication and testing processes, the amount of waste arising from failed experiments and fabrication was significantly reduced. The first application of these GNPs to the LFA revealed that the modification successfully removed the problems with quantifying BPA and effectively decreased the BPA LOD toward the instrument detection level.

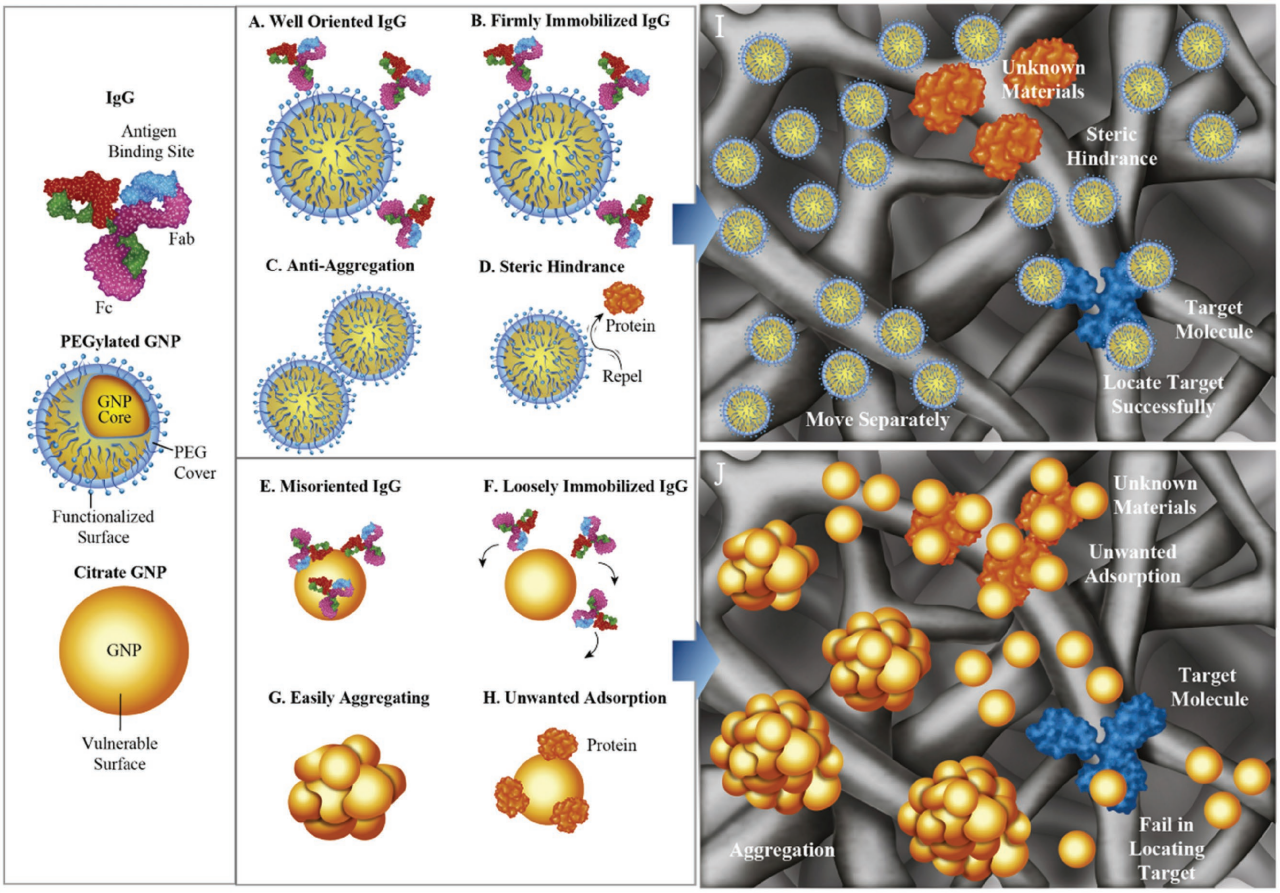

Figure 1. Schematic illustration of the comparison of customized PEGylated GNPs and citrate GNPs. A) Functionalized surfaces orient the antibodies on the surfaces. B) Antibodies are firmly fixed on the surfaces by EDC/NHS chemistry. C) PEG layer prevents the particles from aggregating. D) Steric hindrance decreases nonselective adsorption. E,F) Antibodies are loosely and randomly attached to the surfaces by electrostatic forces. G) GNPs easily aggregate under different conditions. H) Undesirable adsorptions occur frequently. I) The customized particles move separately in a nitrocellulose membrane and successfully conduct target locating and decrease the possibility of false negatives/positives. J) Citrate/regular GNPs aggregate easily in the membrane and increase the possibility of false negatives/positives.

2. Results and Discussion

In this study, we improved on previously reported BPA LFAs by applying customized PEGylated GNPs to LF strips for easier and more stable, reliable, and sensitive quantitative measurements. The design of the modified BPA LFA is shown in **Figure 2**. Initially, we started to develop the modified BPA LFA by investigating citrate GNPs and customized PEGylated GNPs.

Before we applied the customized GNPs to the LFA, the optical properties of modified GNPs should be tuned. The color of the GNPs is decisive in LFA because it determines the signal clarity and sensitivity. First, the optical properties of the regular GNPs were investigated based on Mie theory and reported calculations concerning surface plasmon resonance (SPR). Briefly, the SPR of the GNPs was evaluated by calculating their extinction efficiencies (Q_{ext}), which are composed of the adsorption efficiency (Q_{abs}), including the absorption intensity and the ratio of incident light to light absorption, and the scattering efficiency (Q_{sca}), which includes the scattering intensity and the ratio of incident light to light scattering. These values are expressed as follows[33–35]

$$Q_{ext} = Q_{abs} + Q_{sca} \tag{1}$$

$$Q_{ext} = \frac{2}{x^2}\sum_{n=1}^{\infty}(2n+1)\,\mathrm{Re}\left[a_n + b_n\right] \tag{2}$$

$$Q_{sca} = \frac{2}{x^2}\sum_{n=1}^{\infty}(2n+1)\left[a_n^2 + b_n^2\right] \tag{3}$$

$$a_n = \frac{m\psi_n(mx)\psi_n'(x) - \psi_n(x)\gamma_n'(mx)}{m\psi_n(mx)\xi_n'(x) - m\xi_n(x)\psi_n'(mx)} \tag{4}$$

$$b_n = \frac{\psi_n(mx)\psi_n'(x) - m\psi_n(x)\gamma_n'(mx)}{\psi_n(mx)\xi_n'(x) - m\xi_n(x)\psi_n'(mx)} \tag{5}$$

where $m = \frac{n\,(\text{sphere})}{n_m\,(\text{medium})}$, n is the refractive index, ψ_n, ξ_n are the Riccati–Bessel functions, and $x = \frac{2\pi n_m R}{\lambda}$.

According to Equations (1)–(5), 40 nm diameter GNPs displayed the highest optical absorption at the optical resonance wavelength (λ_{max}), which was approximately 520 nm. GNPs

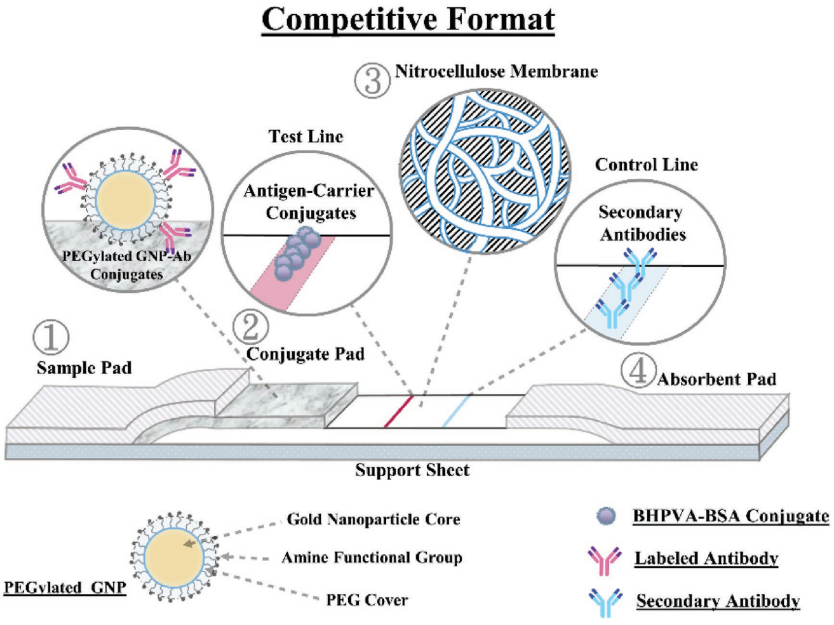

Figure 2. Scheme of the modified PEGylated GNPs applied to a BPA LFA.

with the strongest adsorption close to the ultraviolet wavelength were expected to generate the most scattered light with wavelengths in the infrared region. In addition, we had observed a bright red color for 40 nm citrate GNPs, which were obtained by reduction with citrate. The size changes in the GNPs caused inadequate red/blueshifts in the spectra and fainter color variations, which are unfavorable for our modified BPA LFA.

The HF 120 membrane employed was also assessed before evaluating the regular and customized GNPs. Scanning electron microscope (SEM) images revealed the presence of pores between 100 and 20 μm in size, formed by cellulose in the HF 120 nitrocellulose membrane. Thus, the optimal size of the GNPs to facilitate flow in the membrane was less than 100 nm.

After the analysis of the regular GNPs, the PEG layer on the modified GNPs was investigated because the above equations show that the surrounding environment and adsorbed materials on particle surfaces have significant effects on the color of the GNPs. Thus, 40 nm PEGylated GNPs coated with PEG 1000, 3000, 5000, 7000, or 10000 were assessed, and the PEGylated GNPs coated with PEG 5000 were selected. The PEGylated GNPs coated with PEG 1000 or 3000 exhibited weaker antiaggregation abilities, whereas the GNPs coated with PEG 7000 or 10000 have a poor flowing ability in the LFA and have colors that were shifted from red. After the defined PEG chain was selected, the optical properties of the customized PEG 5000-coated GNP with sizes of 5, 15, and 40 nm were analyzed before being applied to the LFA. Redshift behavior similar to that of regular GNPs was observed as the sizes of the customized GNPs were increased. The customized PEG 5000-coated GNPs of 40 nm in diameter show a brighter red color, which is much more suitable for LFA. Therefore, because of the optical properties and flowing ability of the GNPs in the membrane, 40 nm regular and customized GNPs were adopted for the additional LFA studies, and 5, 15, and 40 nm customized GNPs were used to ensure the stability of the customized PEGylated GNPs.

Additionally, the existence of a PEG layer on the GNP surface was examined using a transmission electron microscope (TEM). The PEGylated GNPs exhibited a coating of ≈1 nm in thickness as "*t*," whereas the citrate GNPs displayed no outer layer around the particles.

To further confirm the presence of the PEG layer on the particles, PEG-covered GNPs and PEG-uncovered GNPs treated with negative stain were observed using TEM (**Figure 3**). The

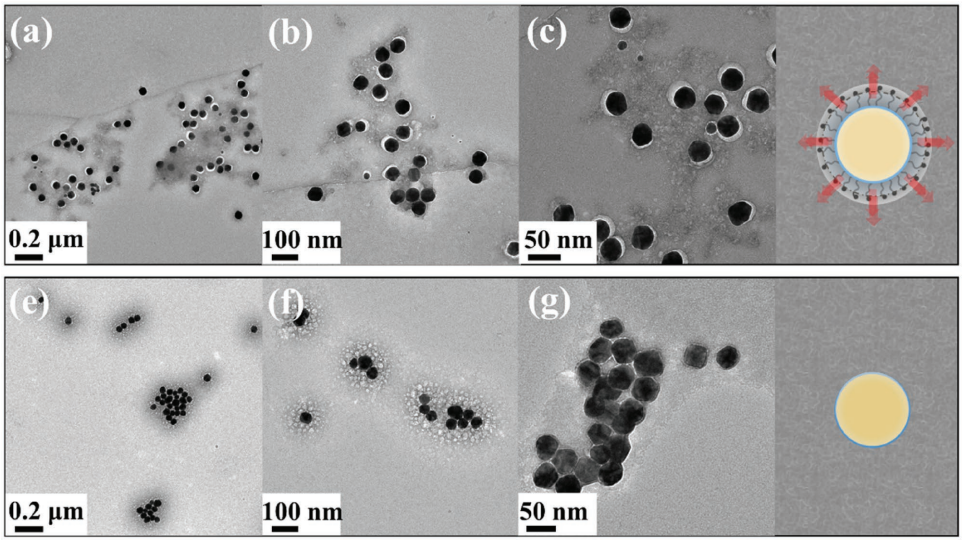

Figure 3. Negative stain TEM images of a–c) 40 nm PEGylated GNPs and e–f) 40 nm citrate GNPs.

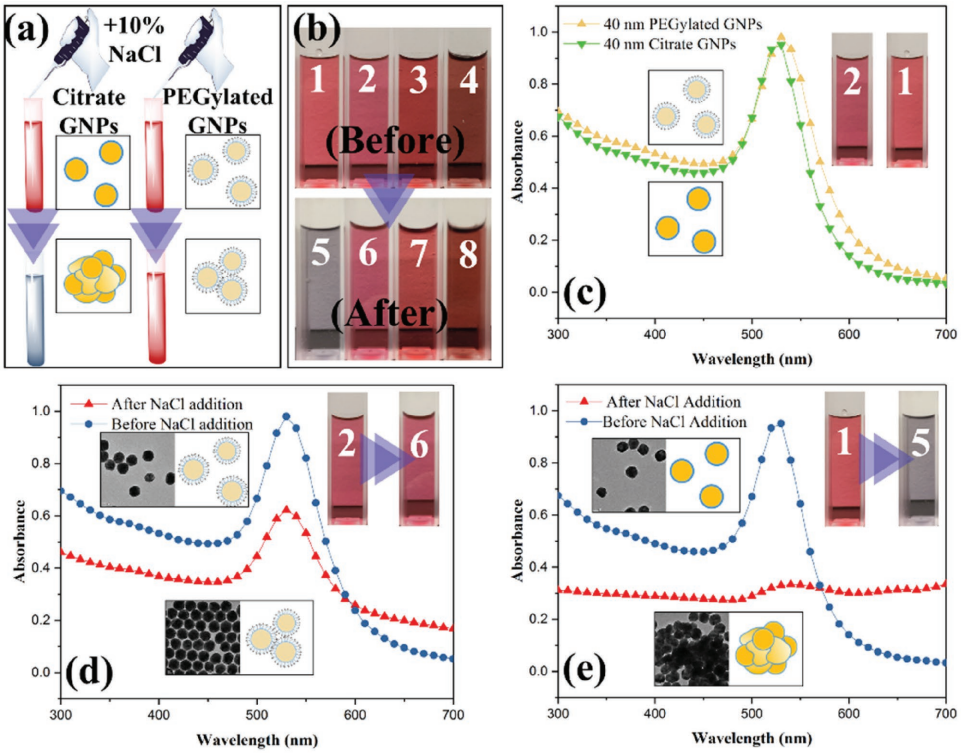

Figure 4. The stability evaluation of the PEGylated GNPs (numbers 2, 3, 4, 6, 7, and 8) and citrate GNPs (numbers 1 and 5) following the addition of 10% NaCl, as determined by UV–vis spectroscopy and TEM. a) Scheme of the changes in the PEGylated GNPs and citrate GNPs before and after the addition of 10% NaCl. b) The appearance changes resulting from GNP aggregation in the PEGylated GNPs before and after the addition of 10% NaCl (before: numbers 2, 3, and 4; after: numbers 6, 7, and 8) and citrate GNPs (before: number 1; after: number 5). c) Absorption spectra of the 40 nm PEGylated GNPs (brown line) and 40 nm citrate GNPs (green line). d) Absorption spectra and TEM images of the 40 nm PEGylated GNPs before (blue line) and after (red line) adding 10% NaCl. e) Absorption spectra and TEM images of the 40 nm citrate GNPs 40 nm before (blue line) and after adding 10% NaCl.

TEM images of the PEGylated GNPs showed that around the gold core a white ring arising from the stain-repelling effect of the PEG layer was present, whereas the images of the citrate GNPs exhibited GNP cores coated by stains.

Many LFAs, including BPA LFAs, are conducted in buffers to render the environment suitable for the biocomponents used in assays. However, common buffers contain a certain amount of salts (e.g., phosphate buffered saline (PBS) contains 0.138 M NaCl), which increase the ion concentration in solutions. Increasing the ion concentration induces the instability and aggregation of GNPs. Therefore, before the GNPs were applied to the LFA, the stability of both the PEGylated GNP and citrate GNPs was evaluated and compared by adding 10% NaCl (100 µL) (**Figure 4**) to replicate the high salt buffer environment in the cellulose membrane. As shown in Figure 4b–e, the citrate GNPs aggregated within 3 min, whereas the customized GNPs were still separated. After the addition of 10% NaCl, the absorption of the citrate GNPs mostly shifted away from the visible light region because the citrate GNPs adhered to each other and formed larger particles, whereas the absorption of the customized GNPs remained in the range of original wavelength with only a slight reduction. This observation was ascribed to the customized GNPs remaining separated and to a reduction in interparticle distances. The zeta potential readings of citrate GNPs (40 nm) drastically changed from −36 to −4 mV while PEG GNPs (5, 15, and 40 nm) only reduced slightly to 9, 8, 6 mV, respectively, after the addition of 10% NaCl. Our subsequent experiments in which we added BSA as a blocking agent to stabilize the citrate GNPs showed similar levels of aggregation after the addition of NaCl. The results demonstrated that the citrate GNP suffered from aggregation during the LF tests, whereas the customized PEGylated GNP were undisturbed by ion concentration while the sample was flowing through the membrane.

After the stability evaluation and optical property tuning, the PEGylated GNPs were applied to the BPA lateral flow tests as an experiment group (I), whereas the citrate GNPs with the BSA blocking agent on their surfaces, as previously reported,[16] were also applied in the BPA lateral flow tests (II) as a control group (**Figure 5**). Figure 5a shows that group II showed a strong reddish color outside of the control and testing regions (i.e., the background area), whereas group I displayed no color in the background areas. The difference in the reddish color (optical density) in the background area on the membranes of groups I and II stemmed from the difference in solubility in aqueous solution and in propensity to aggregate between the PEGylated GNPs and citrate GNPs. Compared to the customized PEGylated GNPs, citrate GNPs were more insoluble in aqueous solution and were more likely to move separately from water and aggregate while a sample was flowing through the

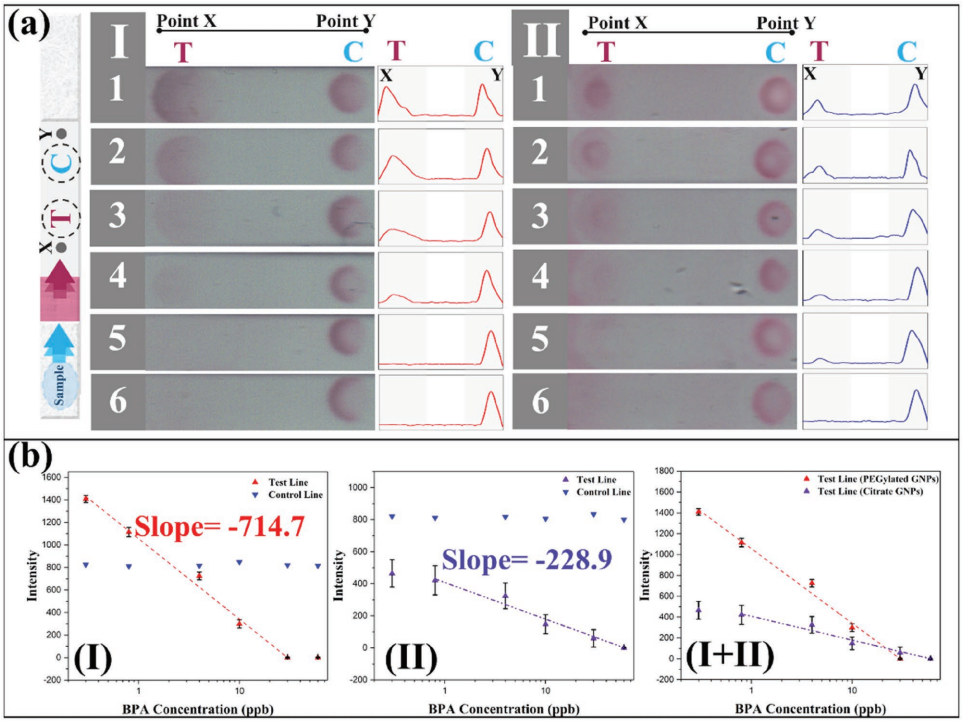

Figure 5. Comparison of the modified BPA LFA (with the customized PEGylated GNPs, I) and regular BPA LFA (with the citrate GNPs, II) using different BPA concentrations conducted in PBS solution. 1) Negative, 2) 0.0008 μg mL^{-1} = 0.8 ppb, 3) 0.004 μg mL^{-1} = 4 ppb, 4) 0.01 μg mL^{-1} = 10 ppb, 5) 0.03 μg mL^{-1} = 30 ppb, and 6) 0.06 μg mL^{-1} = 60 ppb. Each intensity value is the average of three measurements.

membrane. The PEG layers firmly fixed through thiols to the surfaces of the customized GNPs enabled the particles to move together with sample solutions due to their increased solubility and prevented the particles from aggregating during flow, which resulted in almost no optical density in the background area. In addition, the LOD of the modified BPA LFA was remarkable. The naked-eye LOD was defined as the lowest concentration of antigen at which the difference between the intensity of the negative control strip and that of the test strip could be distinguished. In group I, compared to negative strip number 1, the intensity and size of the testing area on strip number 2 were discernible, resulting in a 0.0008 μg mL^{-1} naked-eye LOD. In group II, differentiating between strips 1, 2, and 3 is difficult without the use of a high-resolution scanner. Consequently, the naked-eye LOD was defined as strip number 4, which corresponded to a 0.01 μg mL^{-1} BPA concentration. The naked-eye LOD for group I was 12.5 times greater than that for group II. Furthermore, calibration curves for both groups I and II were generated by determining the intensities in peak areas and are shown in Figure 5b. The two calibration curves show that the slope of the calibration curve for group I is three times greater than that of the calibration line for group II, which indicates that the modified BPA LFA had a higher sensitivity toward BPA. This result was due to the combination of the intensities in both the testing and background areas. The quantitative LOD of the modified BPA LFA obtained using a high-resolution scanner was 0.000472 μg mL^{-1}, whereas the quantitative LOD of regular BPA LFA was only 0.00109 μg mL^{-1}. Here, the quantitative LOD is defined as the BPA concentration causing a 10% reduction in intensity compared to the intensity of a negative strip.[36] Notably, the calibration curve of the modified BPA LFA was much more accurate at lower BPA concentrations than that of the regular BPA LFA.

After the comparison between the BPA lateral tests using the modified GNPs and citrate GNPs, the nonspecific adsorptions on the GNP surfaces were evaluated by making an extra control line (control line 1) in the nitrocellulose membrane with antimouse Ab, which could not react with rabbit anti-BPA Abs on the surfaces of both the modified and regular GNPs. Control line 1 was located between the test line and the regular control line (control line 2) (**Figure 6**). The tests were performed by dropping a BPA-free sample onto the sample pad and observing the GNP surface adsorptions. The tests were conducted with 10 strip tests each for both the modified BPA LFA and regular BPA LFA, and each set was repeated three times (30 strip tests in total for each). In our experience, the intensity of the control line varies with the concentration of anti-BPA Ab on the gold surfaces; therefore, the control line intensities of both the modified BPA LFA and regular BPA LFA in Figures 5 and 6 and the number of Abs on the surfaces of both the modified GNPs and citrate GNPs were adjusted to be the same. In these tests, the modified BPA LFA showed 100% of the results shown in A, whereas the regular BPA LFA with the BSA blocking agent showed 73.3% of the results shown in B plus 26.6% of the results shown in C. These results indicated a 26.6% possibility of nonselective adsorption on the surfaces of citrate GNPs with the BSA blocking agent, whereas the modified GNPs without any blocking agent on their surfaces showed no unwanted

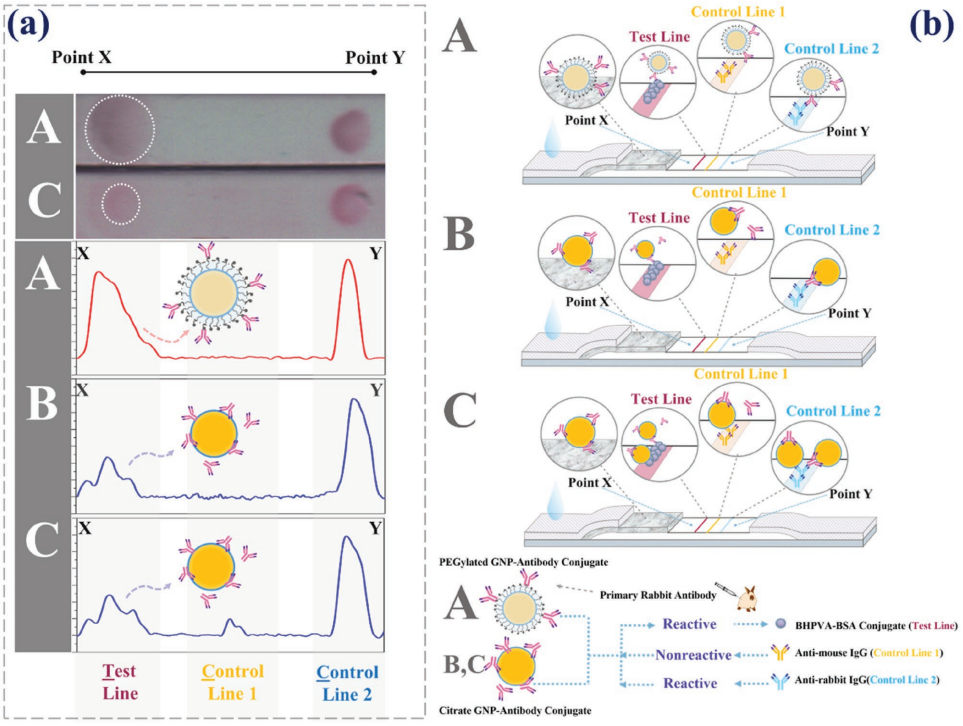

Figure 6. The unwanted (nonselective) adsorption tests and the evaluation of Ab orientations on the GNP surfaces of A) the modified BPA LFA and B,C) regular BPA LFA (B (73.3%) and C (26.6%)). a) Strip images and signal intensity profiles of the modified BPA LFA and regular BPA LFA. b) Theoretical explanations for the sensitivity of A) the modified BPA LFA compared to that of B,C) the regular BPA LFA (B (73.3%) and C (26.6%)).

adsorption. In addition, according to the antibody structure, a lysine residue is encoded in the C-terminal clipping of heavy-chain genes, which is called "C-terminal lysine clipping."[37–41] The orientation of the Abs on the modified GNPs could be analyzed by comparing the images of the strips in Figure 6a to the calibration curves in Figure 5b. Because the Abs on the surfaces of the modified GNPs were favorably oriented by 1-ethyl-3-(3-dimethyl-aminopropyl)-carbodiimide · HCl (EDC)/N-hydroxy-succinimide (NHS) chemistry, they were better able to catch the antigen in the testing area, as shown in A, than those shown in C, resulting a larger signal area of the testing line in A than in C. The calibration curves in Figure 5b revealed that the number of anti-BPA Abs on the modified GNPs was approximately equal to the number of anti-BPA Abs on citrate GNPs, indicating the more effective and efficient antibody–antigen (Ab–Ag) binding performance for the Abs on the modified GNPs.

In addition, the selectivity of the modified BPA LFA was evaluated using common chemicals with similar structures to BPA,

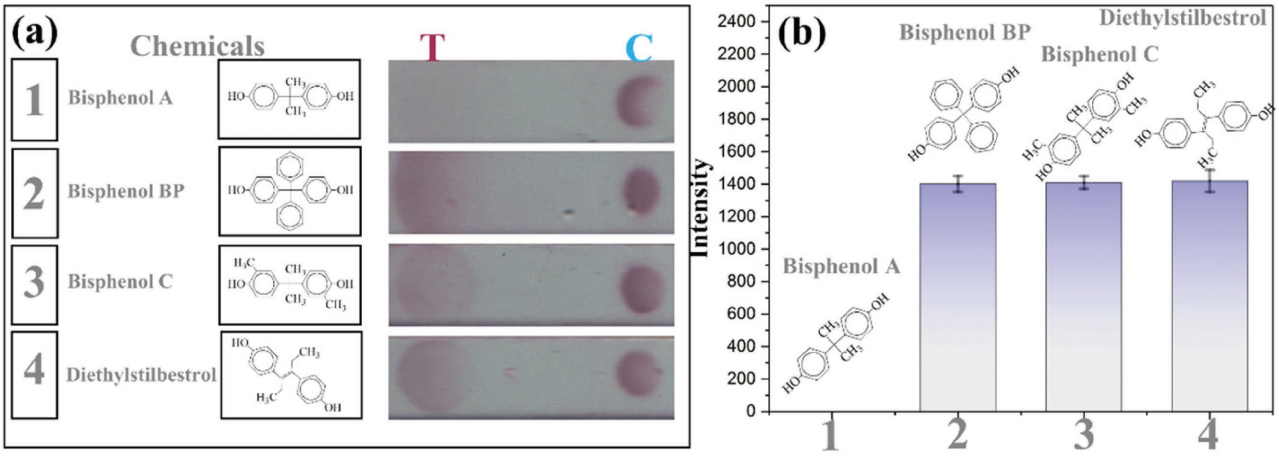

Figure 7. Evaluating the selectivity of the modified BPA LFA. Tested chemicals (0.1 μg mL^{-1} = 100 ppb): 1) BPA, 2) bisphenol BP, 3) bisphenol C, and 4) diethylstilbestrol.

Table 1. Spike and recovery test for modified BPA LFA using real tap water samples.

Tap water samples ($n = 3$ per sample)	Spiked concentration [ppb]	Found concentration [ppb]		Relative standard deviation	Recovery [%]
		Visual[a)]	Quantification analysis		
Number 1	0.8		0.78	2.8	97.5
Number 2	4		3.65	4.6	91.3
Number 3	10		10.67	1.7	106.7
Number 4	20		20.63	3.4	103.2
Number 5	30		29.85	2.5	99.5

[a)]Visual positive/negative identification: negative positive.

including bisphenol BP, bisphenol C, and diethylstilbestrol. The concentrations of all these chemicals were adjusted to 0.1 μg mL^{-1}. **Figure 7** shows that even high concentrations of bisphenol BP, bisphenol C, and diethylstilbestrol could not decrease the intensity in the testing areas, which indicated that the modified BPA LFA is highly specific for BPA.

Finally, the practical value of the modified BPA LFA was examined by a spike and recovery test with real tap water samples (**Table 1**). In this experiment, known amounts of different concentrations of BPA were spiked in tap water (sample numbers 1–5). This result showed a good agreement with those of the BPA samples in PBS solution, which proved that our modified BPA LFA can be used to determine the presence of BPA in the environment.

3. Conclusion

The limitations of naked GNPs lead to enormous losses of valuable materials and make established LF products unstable and unsuitable for long-term use. Therefore, in this study, an advanced BPA LFA with GNPs modified with a firmly fixed PEG layer decorated with extra functional groups was developed and displayed many advantages for BPA detection. The PEG molecules induced steric hindrance on the nanoparticle surface, increased the solubility of the GNPs in aqueous solutions, and reduced nonselective adsorptions. In addition, the outer functional groups could be used to bind Abs via EDC/NHS chemistry, which oriented Abs directionally and increased the Ab–Ag binding efficiency. These benefits from the PEG layer drastically decreased the background signals of the BPA LFA, improved the flowing ability of the GNPs in the membranes, reduced the probability of false negatives/positives, eliminated the instability that might arise from the use of regular GNPs, and increased the sensitivity of the assay. Without the use of any enhancement strategy, the naked-eye LOD was considerably improved to 0.8 ng mL^{-1}, an increase of 12.5 times compared to the regular BPA LFA; moreover, the quantitative LOD was 0.472 ng mL^{-1}, an increase of three times compared to the regular BPA LFA. Notably, although the PEGylated GNPs were applied to the detection of BPA in this work, the application of customized particles to LFA could be extended to any kind of pathogen. We believe that this study will successfully open up new opportunities for advanced LFA applications.

4. Experimental Section

Materials: The LF components, i.e., the cellulose sample/absorbent pad, glass fiber conjugate pad, nitrocellulose membranes, support sheet, and goat antimouse Ab, were purchased from EMD Millipore Corp. (Billerica, MA, USA). Rabbit anti-BPA Ab was purchased from LifeSpan Biosciences (Seattle, WA, USA), Inc. Goat antirabbit Ab was purchased from Fitzgerald Ind. Intl. (Acton, MA, USA). Citrate-capped GNPs and customized PEGylated GNPs were synthesized by Nanopartz Inc. (Loveland, CO, USA). To control the quality and accuracy, all the GNPs and Abs used in this study originated from the same batches. Ultrapure water (>18.3 MΩ), which was used to prepare all the solutions in this study, was obtained from a NANOpure Infinity Unit from APS Water Services Corp. (Van Nuys, CA, USA). All other chemical reagents, which were of analytical grade, and dialysis membranes used in this study were obtained from Sigma-Aldrich Co. (St. Louis, MO, USA). All beakers and glassware were from VWR Intl. (Batavia, IL, USA) and were cleaned with aqua regia composed of a three-to-one ratio of HCl to HNO_3 and washed with ultrapure water before use. The buffer used in this study was a PBS standard solution (10×10^{-3} M, pH 7.4).

Instruments: Images of the citrate and PEGylated GNPs were acquired and analyzed using a Tecnai G2 20 TEM (ACC V: 200 kV) (FEI Corp., Hillsboro, OR, USA). The images of the nitrocellulose membrane were obtained using a Quanta 3D FEG Dual-beam SEM. GNP sizes and zeta potential values were obtained using a Zetasizer Nano Z (Malvern Instruments Ltd., Westborough, MA, USA). The optical densities of the citrate GNPs, PEGylated GNPs, bioconjugates, and Abs were determined using a SpectraMax Plus 384 (Molecular Devices, L.L.C., Sunnyvale, CA, USA). Bioconjugates were freeze-dried using a REVO R&D Freeze Dryer (Purdue Lyophilization Consortium, Millrock Technology Inc., Kingston, NY, USA). Washing and separation procedures were executed using Eppendorf MiniSpin Plus microcentrifuges (Fisher Scientific Co. L.L.C., Schaumburg, IL, USA). XPS spectra of the PEGylated GNPs were obtained by Nanopartz using a Thermo Scientific K-Alpha XPS spectrometer (Thermo Scientific Co. Grand Island, NY, USA).

BPA Solutions: BPA standard powder from Sigma-Aldrich (≥99%) was used to prepare the BPA solutions. The solutions with different concentrations were prepared by dissolving BPA powder in PBS solution (10×10^{-3} M). The samples were stored at 25 °C before use. The concentrations of the stored solutions were confirmed using HPLC.

Labels—PEGylated GNPs and Citrate GNPs: Citrate-capped GNPs with diameters ranging from ≈30 to 100 nm for optical property analysis were synthesized by reducing 5 mL of 0.1% (w/v) $HAuCl_4$ with varying amounts of 1% (w/v) trisodium citrate in ultrapure water. The 40 nm GNPs were used in the LFA because of their more intense color. PEGylated GNPs coated with PEG 1000, 3000, 5000, 7000, or 10000 were examined on the homemade GNPs to optimize PEG chains applied on LFA. A reported method with minor modifications was applied for the PEG coating process. An optimized amount of PEG-SH was dropped into GNP solution (≈0.12×10^{-9} M, 1 mL). The solution was then stirred for 2 h and maintained at 4 °C for 12 h.[42] A centrifugal

washing process at 14.1 rcf was then adopted to remove unbound PEG-SH. The PEGylated GNPs coated with PEG 5000 were finally selected for the BPA LFA study because of their adequate stability and decreased optical interference from the PEG chains. To accurately compare the customized 40 nm PEGylated GNPs with the commercial 40 nm citrate GNPs purchased from Nanopartz Inc., both were applied on LF strips. The customized PEGylated GNPs are composed of a GNP core fully covered with customized polymer structures (HS-PEG 5000-NH_2) to provide improved particle stability and additional covalent binding sites. All the homemade and purchased GNPs were stored at 4 °C before use.

Preparation of BHPVA–BSA Conjugate: 4,4-bis(4-hydroxyphenyl) valeric acid to bovine serum albumin (BHPVA-BSA) is an artificial antigen-carrier conjugate. It is commonly used as the hapten conjugate for fabricating anti-BPA Ab. BHPVA-BSA was synthesized according to a reported method with a few modifications and made into a compete antigen in the testing area of the LF strips. Briefly, BHPVA was connected to BSA using EDC/NHS chemistry. Initially, BHPVA, NHS, and EDC at a molar ratio of 1:1.25:1.25 were mixed together and were magnetically stirred for 2 h to activate BHPVA. The activated BHPVA solution was then mixed with BSA dissolved in $NaHCO_3$ solution (0.1 mol L^{-1}), which had previously been adjusted to pH 7 with HCl, to obtain the final mixture. The hydrophilicity of the final mixture was affected by the amount of activated BHPVA. Excess BHPVA interfered with the interaction between the flowing sample and the conjugate on the lateral membrane. To remove unbound BHPVA molecules, the optimized final mixture was then dialyzed against PBS and ultrapure water for 24 and 48 h, respectively. The dialysis process was conducted in a refrigerator at 4 °C. The purified product was finally freeze-dried using a REVO freeze dryer to afford a white powder, which was stored at −20 °C. The stored powder was weighed and dissolved in PBS solution (10×10^{-3} M) before use.[43]

Preparation of Citrate GNP–Ab Conjugate: The citrate GNP–Ab conjugates that were compared with the PEGylated GNP–Ab conjugates were prepared according to a previously reported method with some modifications. First, the commercial rabbit anti-BPA Ab was diluted in PBS (10×10^{-3} M) at pH 7.4 to different concentrations. Because of the competitive format applied in this study, different concentrations of anti-BPA Ab were added to the 40 nm citrate GNP solution at a pH value of 8.0, adjusted by Na_2CO_3 (0.1 M), to define the optimal amount of Ab to maintain nanoparticle stability and to detect low concentrations of BPA. After the optimization process, a well-defined concentration of anti-BPA Ab was then added to GNP solution (1 mL) to prepare the citrate GNP–Ab conjugates, and the solution was magnetically stirred for 1 h. Next, BSA (0.1 mL) was added to the solution and magnetically stirred for 0.5 h. The GNP–Ab conjugates were then separated from the solution by centrifugation at 14.1 rcf for 15 min, and the deposits were resuspended into an aqueous solution containing 1% BSA, 1% Tween 20, 5% sucrose, and 0.02% sodium azide (w/v). The conjugates were stored at 4 °C.[27]

Preparation of PEGylated GNP–Ab Conjugate: Except for the covalent binding and hydrophobicity-removal steps, the main washing and separation steps of the PEGylated GNP–Ab conjugates were equivalent to those of the citrate GNP–Ab conjugates for comparison. Before the process, the zeta potentials of the PEGylated GNPs were examined to ensure that the amine groups on the particle surface are stable. Equivalent to the first step for the citrate GNP–Ab conjugates, the optimal concentration of the Ab was defined beforehand. The optimal concentration of the Ab for PEGylated GNP–Ab bindings was different than that for citrate GNP–Ab bindings because the PEG layer repelled a large portion of Abs from attaching. The optimal concentration of the anti-BPA antibody diluent was prepared from 0.8 mg mL^{-1} and varied depending on the species, quality, and health of the antibody. Then, the PEGylated GNPs were mixed with the well-defined Ab (70 µL) and the crosslinkers NHS and EDC in a 1:1 molar ratio. The reaction was conducted under magnetic stirring for 2 h to form crosslinks between the amine groups on the surface of PEGylated GNPs and the C-terminal of the anti-BPA Ab. Next, BSA (0.2 mL) and Tween 20 (0.36 mL) were added to the solution and stirred for 0.5 h. The GNP–Ab conjugates were then separated from the solution by centrifugation at 14.1 rcf for 30 min, and the pellets were resuspended and stored as described for the citrate GNP–Ab conjugates.

Modified BPA LFA: Several elements of the modified BPA LFA, namely, the sample pad (1), conjugate pad (2), nitrocellulose membrane (3), and absorbent pad (4), were laminated and held together by a support sheet (Figure 2). The strip dimensions were 58 mm × 4 mm. Each part was overlapped by 3 mm to ensure sample transport between pads. For the nitrocellulose membrane, HF 075, HF 090, HF 120, HF 135, and HF 180 were tested, and HF 120 was selected as the optimal membrane because of the high sensitivity of the membrane and decreased adhesion of the PEGylated GNPs to the membrane. The 0.68 mm thick sample pads composed of cellulose C083 were cut into 18 mm × 4 mm pieces. The 0.43 mm thick conjugated pad was composed of glass fiber G041 cut into 8 mm × 4 mm pieces. A single drop of BHPVA-BSA solution (1 µL) and a single drop of goat antirabbit Ab (1 µL) were added onto the virtual test line and the virtual control line, respectively, on the nitrocellulose membrane using an automatic pipette. The anti-BPA Ab covalently bound to the PEGylated GNPs was dispersed onto the conjugate pad. The finished products were dried and stored at 4 °C.

Data Acquirement and Analysis: Repeated triplicate measurements were adopted for every parameter in this study. LF strip intensities were acquired within 15 min after each measurement using a Canon high-resolution scanner and were processed using ImageJ. The acquired data are shown as the mean values with standard deviations. All spectral and intensity data were analyzed using OriginPro 2017 (Northampton, MA, USA). The strip signals in this study are defined as the grayscale value of the test line/control line ($S_{Test}/S_{Control}$) and the grayscale value of the background area ($S_{Background}$). The intensity of the test and control lines was defined by the integrated peak area of the test/control line signals. The values were determined using Equations (6) and (7)

$$\text{Test line signal} = S_{Test} - S_{Background} \quad (6)$$

$$\text{Control line signal} = S_{Control} - S_{Background} \quad (7)$$

Supporting Information

Supporting Information is available from the Wiley Online Library or from the author.

Acknowledgements

The authors acknowledge the support of LyoHUB demo facility at Birck Nanotechnology Center, and the help of Professor Alina Alexeenko and her student, Andrew Strongrich, from the School of Aeronautics and Astronautics.

Conflict of Interest

The authors declare no conflict of interest.

Keywords

BPA, immunochromatographic assays, lateral flow, PEGylated nanoparticles

Received: August 16, 2017
Revised: October 13, 2017
Published online:

[1] L. N. Vandenberg, M. V. Maffini, C. Sonnenschein, B. S. Rubin, A. M. Soto, *Endocr. Rev.* **2009**, *30*, 75.
[2] G. D. Bittner, C. Z. Yang, M. A. Stoner, *Environ. Health* **2014**, *13*, 41.
[3] M. Lorber, A. Schecter, O. Paepke, W. Shropshire, K. Christensen, L. Birnbaum, *Environ. Int.* **2015**, *77*, 55.
[4] T. J. Murray, M. V. Maffini, A. A. Ucci, C. Sonnenschein, A. M. Soto, *Reprod. Toxicol.* **2007**, *23*, 383.
[5] A. C. Gore, *Endocrine-Disrupting Chemicals: From Basic Research to Clinical Practice*, Humana Press, Totowa, NJ **2007**.
[6] M. Wu, C. Pan, M. Yang, B. Xu, X. Lei, J. Ma, L. Cai, J. Chen, *Environ. Toxicol. Chem.* **2016**, *35*, 182.
[7] P. Deb, A. Bhan, I. Hussain, K. I. Ansari, S. A. Bobzean, T. K. Pandita, L. I. Perrotti, S. S. Mandal, *Gene* **2016**, *590*, 234.
[8] D. D. Seachrist, K. W. Bonk, S. M. Ho, G. S. Prins, A. M. Soto, R. A. Keri, *Reprod. Toxicol.* **2016**, *59*, 167.
[9] S. Biedermann-Brem, K. Grob, *Eur. Food Res. Technol.* **2009**, *228*, 679.
[10] A. M. Hormann, F. S. vom Saal, S. C. Nagel, R. W. Stahlhut, C. L. Moyer, M. R. Ellersieck, W. V. Welshons, P. L. Toutain, J. A. Taylor, *PLoS One* **2014**, *9*, 1.
[11] S. M. Zimmers, E. P. Browne, P. W. O'Keefe, D. L. Anderton, L. Kramer, D. A. Reckhow, K. F. Arcaro, *Chemosphere* **2014**, *104*, 237.
[12] Y. Gibert, I. ebrary, *Bisphenol A: Sources, Risks of Environmental Exposure and Human Health Effects*, Nova Science, Hauppauge, NY **2015**.
[13] E. Chung, J. Jeon, J. Yu, C. Lee, J. Choo, *Biosens. Bioelectron.* **2015**, *64*, 560.
[14] J. Feng, L. Xu, G. Cui, X. Wu, W. Ma, H. Kuang, C. Xu, *Biosens. Bioelectron.* **2016**, *81*, 138.
[15] J. G. Hengstler, H. Foth, T. Gebel, P.-J. Kramer, W. Lilienblum, H. Schweinfurth, W. Völkel, K.-M. Wollin, U. Gundert-Remy, *Crit. Rev. Toxicol.* **2011**, *41*, 263.
[16] Z. Mei, H. Chu, W. Chen, F. Xue, J. Liu, H. Xu, R. Zhang, L. Zheng, *Biosens. Bioelectron.* **2013**, *39*, 26.
[17] Y. Lei, Q. Zhang, L. Fang, M. S. H. Akash, K. Rehman, Z. Liu, W. Shi, S. Chen, *Drug Test. Anal.* **2014**, *6*, 1020.
[18] D. Zhang, J. Yang, J. Ye, L. Xu, H. Xu, S. Zhan, B. Xia, L. Wang, *Anal. Biochem.* **2016**, *499*, 51.
[19] R. Wong, *Lateral Flow Immunoassay*, Humana Press, Totowa, NJ **2008**.
[20] M. Sajid, A. N. Kawde, M. Daud, *J. Saudi Chem. Soc.* **2015**, *19*, 689.
[21] D. Quesada-González, A. Merkoçi, *Biosens. Bioelectron.* **2015**, *73*, 47.
[22] W. Wu, S. Zhao, Y. Mao, Z. Fang, X. Lu, L. Zeng, *Anal. Chim. Acta* **2015**, *861*, 62.
[23] J. V. Samsonova, V. A. Safronova, A. P. Osipov, *Talanta* **2015**, *132*, 685.
[24] C. Zheng, X. Wang, Y. Lu, Y. Liu, *Food Control* **2012**, *26*, 446.
[25] I. H. Cho, A. Bhunia, J. Irudayaraj, *Int. J. Food Microbiol.* **2015**, *206*, 60.
[26] B. Y. Moghadam, K. T. Connelly, J. D. Posner, *Anal. Chem.* **2015**, *87*, 1009.
[27] Z. Mei, W. Qu, Y. Deng, H. Chu, J. Cao, F. Xue, L. Zheng, H. S. El-Nezamic, Y. Wu, W. Chen, *Biosens. Bioelectron.* **2013**, *49*, 457.
[28] E. Maiolini, E. Ferri, A. L. Pitasi, A. Montoya, M. D. Giovanni, E. Errani, S. Girotti, *Analyst* **2013**, *139*, 318.
[29] M. R. Hormozi-Nezhad, S. Abbasi-Moayed, *Plasmonics* **2015**, *10*, 971.
[30] M. Ijeh, *Ph.D. Thesis*, Hamburg University, Germany **2011**.
[31] E. Jue, C. D. Yamanishi, R. Y. T. Chiu, B. M. Wu, D. T. Kamei, *Biotechnol. Bioeng.* **2014**, *111*, 2499.
[32] K. Ling, H. Jiang, Q. Zhang, *Nanoscale Res. Lett.* **2013**, *8*, 538.
[33] G. Mie, *Ann. Phys.* **1908**, *25*, 377.
[34] X. Huang, M. A. El-Sayed, *J. Adv. Res.* **2010**, *1*, 13.
[35] P. K. Jain, K. S. Lee, I. H. El-Sayed, M. A. El-Sayed, *J. Phys. Chem. B* **2006**, *110*, 7238.
[36] H. Xie, W. Ma, L. Liu, W. Chen, C. Peng, C. Xu, L. Wang, *Anal. Chim. Acta* **2009**, *634*, 129.
[37] A. Beck, T. Wurch, C. Bailly, N. Corvaia, *Nat. Rev. Immunol.* **2010**, *10*, 345.
[38] F. Higel, A. Seidl, F. Sörgel, W. Friess, *Eur. J. Pharm. Biopharm.* **2016**, *100*, 94.
[39] H. Liu, G. Gaza-Bulseco, D. Faldu, C. Chumsae, J. Sun, *J. Pharm. Sci.* **2008**, *97*, 2426.
[40] B. Cai, H. Pan, G. C. Flynn, *Biotechnol. Bioeng.* **2011**, *108*, 404.
[41] A. Beck, S. Sanglier-Cianférani, A. V. Dorsselaer, *Anal. Chem.* **2012**, *84*, 4637.
[42] J. Gao, X. Huang, H. Liu, F. Zan, J. Ren, *Langmuir* **2012**, *28*, 4464.
[43] M. P. Zhao, Y. Z. Li, Z. Q. Guo, X. X. Zhang, W. B. Chang, *Talanta* **2002**, *57*, 1205.

